Gandhi, H. S., Shelef, M., *J. Catal.*, **24**, 241 (1972).
Gregg, S. J., Sing, K. S. W., "Adsorption, Surface Area and Porosity", Academic Press, New York, N.Y., 1967.
Hirota, K., Kera, Y., Teratani, S., *J. Phys. Chem.*, **59**, 388 (1955).
Kakati, K. K., Wilman, H., *J. Phys. D, Appl. Phys.*, **6**, 1307 (1973).
Kon, M. Ya., Shvets, V. A., Kazanskii, V. B., "Some Theoretical Problems in Catalyst Research: Report Soviet-Japanese Seminar in Catalysis", p 691, 1971.
Kon, M. Ya., Shvets, V. A., Kazanskii, V. B., *Kinet. Catal. (USSR)*, **13**, 657 (1972).
Kon, M. Ya., Shvets, V. A., Kazanskii, V. B., *Kinet. Catal. (USSR)*, **14**, 339 (1973).
Kon, M. Ya., Shvets, V. A., Kazanskii, V. B., Slovetskaya, K. I., *Kinet. Catal. (USSR)* **15**, 408 (1974).
Lippens, B. C., de Boer, J. H., *J. Catal.*, **4**, 319, 643, 649 (1965).
McHughes, F., Hill, G. R., *J. Phys. Chem.*, **59**, 388 (1955).
Marshneva, V. I., Boreskov, G. K., Soklilovski, V. D., *Kinet. Catal. (USSR)*, **13**, 1209 (1972).
Mitchell, P. C. H., Trifiro, F., *J. Catal.*, **33**, 350 (1974).
Shelef, M., Otto, K., Gandhi, H. S., *J. Catal.*, **12**, 361 (1968).
Shvets, V. A., Kazanskii, V. B., *Kinet. Catal. (USSR)*, **12**, 834 (1971).
Shvets, V. A., Kazanskii, V. B., *J. Catal.*, **25**, 123 (1972).
Shvets, V. A., Sarichev, M. E., Kazanskii, V. B., *J. Catal.*, **11**, 378 (1968).
Shvets, V. A., Vorotynstsev, V. M., Kazanskii, V. B., *Kinet. Catal. (USSR)*, **10**, 287 (1969).
Simmard, G. L., Streger, J. F., Arnott, R. Y., Sigal, L. A., *Ind. Eng. Chem.*, **47**, 1424 (1955).
Sterba, M. J., Haensel, V., *Ind. Eng. Chem. Prod. Res. Dev.*, **15**, 3 (1976).
Stone, F. S., *Adv. Catal.*, **13**, 1 (1962).
Tarama, K., Teratani, S., Yoshida, S., Tamura, N., *Proc. Int. Congr. Catal., 3rd, 1964* (1965).
Thomas, J. M., Thomas, W. J., "Introduction to the Principles of Heterogeneous Catalysis", Academic Press, New York, N.Y., 1967.
Van Reijen, L. L., Cossee, P., *Discuss Faraday Soc.*, **41**, 277 (1966).
Vorotinzev, V. M., Shvets, V. A., Kazanskii, V. B., *Kinet. Catal. (USSR)*, **12**, 597 (1971).
Wyckoff, R. W. G., "Crystal Structures", Vol. 2, Interscience, New York, N.Y., 1966.

Received for review February 13, 1978
Accepted October 2, 1978

GENERAL ARTICLES

Steam Cracking of Hydrocarbons. 1. Pyrolysis of Heptane

Martin Bajus and Václav Veselý

Department of Chemistry and Technology of Petroleum, Slovak Technical University, Bratislava, Czechoslovakia

Piet A. Leclercq and Jacques A. Rijks*

Laboratory of Instrumental Analysis, Eindhoven University of Technology, Eindhoven, The Netherlands

The thermal decomposition of heptane in the presence of steam was studied in a flow reactor with large inner surface. The experiments were performed at atmospheric pressure in a temperature range of 680–760 °C for a mass ratio of steam to hydrocarbon 3:1. The reaction products were analyzed by gas chromatography. For the identification both comparison of retention indices with those of standard compounds and literature data and mass spectrometry were used. The conversion process appeared to be a first-order reaction with a frequency factor of 1.34×10^{11} s^{-1} and an activation energy of 195.5 kJ mol^{-1}. The composition of the mixture of reaction products was in agreement with the Rice–Kossiakoff theory, except for ethane and 1-hexene.

Introduction

The pyrolysis of hydrocarbons from natural gases, refinery gases, or petroleum in tubular reactors between 600 and 900 °C is of prime importance in petrochemical processes. Depending on the charge and working conditions it gives a complex mixture of products from which ethene is the most important. In addition to ethene many olefins and aromatics are found: propene, butenes, butadiene, isoprene, cyclopentadiene, benzene, toluene, xylenes, and styrene. Less valuable products such as methane, heavy pyrolytic naphthas, pyrolytic oils and pyrolytic resins (i.e., hydrocarbons boiling above 140 °C) and coke are formed too.

For optimizing this process the pyrolysis of individual hydrocarbons and of mixtures of hydrocarbons with different properties is frequently studied. It is known that among the pyrolysis products of unbranched alkanes, or naphthas with an alkanic character, ethene and propene prevail. As these are the most valuable products of the pyrolysis it is comprehensible that the kinetics and the mechanism of alkane pyrolysis are most often studied. In the group of alkanes C_5H_{12} to $C_{12}H_{26}$, at about 780 °C, heptane gives the highest conversion and the highest yield of ethene (Bajus and Veselý, 1976). Also in pyrolysis of straight run naphthas, heptane gives the highest conversion. For this reason heptane is particularly suitable for studies of kinetics and mechanisms of the pyrolysis at different reaction rates, and in reaction systems in which wall effects are favorable for the selectivity of the process. This is the case for pyrolysis of naphthas in a stainless steel

0019-7890/79/1218-0030$01.00/0

reactor with a high surface-to-volume ratio, where more ethene, less methane, and less propene are produced than in a quartz reactor working at comparable conditions (Bajus et al., 1977). Of importance is the possibility to totally suppress the formation of higher-boiling oil by decomposing it with steam into hydrogen and carbon monoxide.

The pyrolysis of alkanes at 600 to 900 °C proceeds in a homogeneous phase according to a radical mechanism. The generation of radicals is influenced by wall effects. Surface effects can only be eliminated in a wall-less reactor (Taylor et al., 1969). The wall effects become more apparent when the surface-to-volume ratio is increased. The qualitative and quantitative composition of the product mixture is also influenced by the wall material. It also affects reaction rates which are higher in iron than in quartz or gold reactors (Tamai and Nishiyama, 1970). The tendency to coking is higher in iron, monel, or cobalt than in quartz, porcelain, silver or gold reactors (Hurd and Pilgrim, 1933; Tamai et al., 1967). The views concerning the activation of the inner surface are not in full agreement. According to Crynes and Albright (1969) the surface activation of walls by oxygen, hydrogen, steam, or hydrogen sulfide influences the course of pyrolysis. Marschner (1938) and Kunzru et al. (1972) did not observe this effect.

The deposition of coke on the wall of the reactor is a serious problem in the study of the mechanism and kinetics of the pyrolysis of hydrocarbons. Since coke is mainly deposited on the wall of the reactor there is a continuous change in the surface properties of the reactor. This results in a continuous change of the composition of the reaction products. Cleaning of the reactor by air, oxygen, and steam will also result in a change of the properties of the reactor surface. The reproducibility of the measurements, which requires constant reaction conditions, can be improved by decreasing the partial pressure of the compounds involved in the reaction by addition of an inert diluent. Another possibility is the passivation of the inner surface with surface-active agents.

We chose steam as an inert diluent, as this is currently used in industry. An advantage of steam is its ability to act as reactant under certain conditions. Especially for stainless steel reactors with increased surface, the steam can react with high molecular compounds (or carbon) according to the equation

$$C + H_2O \rightarrow CO + H_2 \quad (1)$$

In this way constant conditions were secured for the pyrolysis of heptane and the equipment could work continuously.

From the analytical techniques that can be applied for the analysis of the products of pyrolysis, gas chromatography (GC) is the most attractive one, mainly for reasons of separation power and the detectability of low concentrations. Gas chromatographic analyses on columns of different polarity and with different detectors yield detailed qualitative information for both gaseous and liquid reaction products, especially when capillary columns are used. This is a great advantage for the study of the mechanism of the reaction. Since gaseous products are dissolved partly in the liquid fraction, this approach will result in a complicated and inaccurate material balance. Therefore, the calculation of the material balance was based on the analysis of all pyrolysis products on one single packed column.

Materials and Methods

I. Pyrolysis Equipment. The equipment used is shown schematically in Figure 1. The flow reactor, made

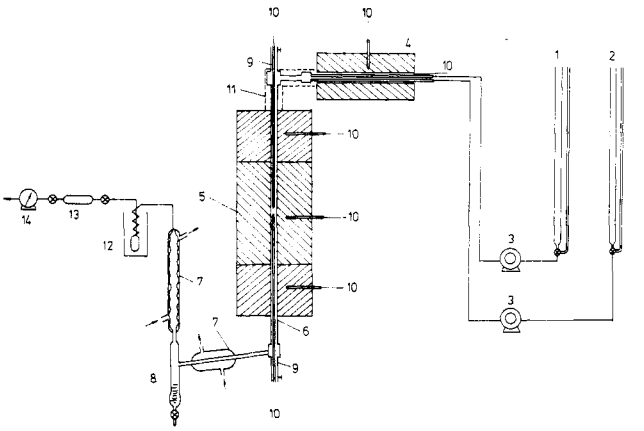

Figure 1. Schematic of the pyrolysis equipment: 1, water container; 2, container for hydrocarbon; 3, pump; 4, preheater; 5, oven; 6, reactor; 7, condenser; 8, separator; 9, thermotube; 10, thermocouple; 11, isolation; 12, cooler; 13, gas sampler; 14, gas meter.

from stainless steel (Czechoslovak standard 17255; composition: 23–27% Cr, 18–22% Ni, max. 2% Si, max. 1.5% Mn, max. 0.25% C) was of the tubular type. The outer tube (length 750 mm; i.d. 12 mm) was placed in an electrically heated furnace. The outside diameter of the inner tube was 6 mm. The inner reactor surface-to-volume ratio was 6.65 cm^{-1}. The pyrolysis reactor had three independently heated sections. The upper and lower section had a power heating of 1.2 kW each, the middle one 2.4 kW, and the preheater 1 kW. The temperature in individual sections was regulated by a regulator of the Zepafot type (ZPA, Nová Paka, Czechoslovakia). The moving Pt–Rh/Rh thermocouples were placed in the inner tube. Glass burets were applied as water and hydrocarbon containers. The products charged to the reactor were measured by the thinner calibrated buret. The continuous charging was performed by micropumps MC-600 (Mikrotechna, Prague, Czechoslovakia). The water and the hydrocarbon were transported from the containers by micropumps into the preheater through polyethene tubing. In the preheater the charge was evaporated at 400 °C in two stainless steel tubes with an inner diameter of 8 mm. From here the charge flowed through a connecting tube into the reactor. The flow of heptane varied from 10 to 35 g h^{-1} and that of water from 30 to 105 g h^{-1}. The reaction products were passed through a water cooler and finally cooled down to −18 °C in a freezing trap.

The purity of heptane (Loba-Chemie Wien, Fischamend), being 99.69%, was determined by gas chromatography. The mass ratio of distilled water and heptane was 3:1 in all experiments.

II. Analytical Instrumentation. The analyses required for the material balance were performed on a CHROM IV gas chromatograph provided with a flame ionization detector (FID), and thermal conductivity detector (TCD) which can easily be exchanged (Laboratorní přístroje, n.p., Prague, Czechoslovakia). The TCD was used for the analysis of hydrogen and carbon monoxide in gaseous samples. The FID was applied for the analysis of the organic compounds in gaseous and liquid products. The experimental conditions are given in Table I.

The precise measurements of retention data were done on a homemade (Rijks and Cramers, 1974) instrument provided with an FID. The separations were carried out on a stainless steel capillary column (length, 100 m; i.d., 0.25 mm). Squalane was used as the stationary phase. The column temperatures were 50 °C and 70 °C ± 0.02 °C. The inlet pressure was 2.5 ± 0.002 atm. The carrier gas was nitrogen or hydrogen. The retention times were

Table I. Analysis of Products of Pyrolysis

	type of analysis			
	1	2	3	4
instrument	CHROM IV	CHROM IV	CHROM IV	homemade
analyzed components	gaseous and liquid products	ethene, ethane	methane, H_2, CO	liquid products
type of column	packed	packed	packed	capillary
length, m	3.7	3.7	2.5	100
internal diameter, mm	3	3	3	0.25
phase (support)	triethene glycol ester of butyric acid	florisil 60/100 mesh	supersorb 0.2-1 mm	squalane
column temperature, °C	25.0-50.0 T.P.[a]	55.0	60.0 T.P.[a]	50.00; 70.00
carrier gas	nitrogen	nitrogen	helium	nitrogen, hydrogen
inlet pressure, Pa	1.01×10^5	1.2×10^5	1.5×10^5	2.5×10^5
size of sample, μL	100 (g); 0.5 (l)	100	100	0.7-1.2

[a] T.P. = temperature programming.

measured either by a stopwatch ("manual registration") or with a digitizer–computer system ("automatic registration").

For a number of compounds identified by table matching of retention indices the identification was confirmed by mass spectrometry (MS), using a GC–MS combination (Leferink and Leclercq, 1974) with the same column.

Quantitative Analysis

The main components in the gaseous fraction of the pyrolysis products of heptane are olefins. In the liquid fraction the main product is the unconverted heptane. The concentrations of the reaction products vary in a wide range. For the overall material balance only the profiling components were taken into account. The trace components formed as intermediate or byproducts and the impurities introduced by heptane were neglected. They are only of interest in the study of the mechanism of pyrolysis.

The organic compounds from both the gaseous and the liquid products were separated on a single packed column and detected by an FID. The concentration of the profiling components was determined according to the equation

$$[a] = \frac{Aa}{\sum_{1}^{n} Ai} \times 100\%$$

The precision of the measurements, which was determined with synthetic calibration mixtures, corresponds to a standard deviation of about 3%. The concentrations of hydrogen, carbon monoxide, and methane were determined by calibration plots (volume vs. area), with a TCD (precision 3–5%).

Qualitative Analysis

The identification of the profiling components in the reaction products, which were separated on packed columns, was done by direct comparison with standard compounds.

To study the mechanism of the pyrolysis of heptane a detailed qualitative analysis is required also for components present in very low concentrations. Since many precise retention data for squalane are available in the literature (Sojâk and Rijks, 1976; Rijks and Cramers, 1974; Hively and Hinton, 1968; Loewenguth and Tourres, 1968; Tourres, 1967), this phase was selected for this study to enable the identification by table matching. For reasons of speed of analysis, in some cases hydrogen was used as the carrier gas instead of nitrogen. With hydrogen the analysis time can be reduced about 50% at the same inlet pressure. The difference in retention index for both gases appeared to be within the experimental error (<0.5 index unit). For retention indices calculated from time measurements with a stopwatch or a digitizer–computer system no significant difference was observed. The retention data of the identified compounds differ only ≤0.3 index unit from the tabulated values. The maximum difference was 1.0 index unit. Considering the peak shift according to incomplete separation of the reaction products these differences can be explained.

With the same column, at the same operating conditions, a GC–MS–computer system was used to confirm the identification by table matching of about 50% of the identified compounds. The results of these investigations are summarized in Table II. The first seven compounds were identified by direct comparison of retention times with those of standards.

Residence Time and Temperature

In order to be able to calculate the effective reactor volume, the temperature profile in the reactor must be known. The longitudinal temperature profile in the reactor is determined mainly by the characteristics of the heating elements, volume velocity, thermal capacities of the reactants and products, and the endothermicity of the reaction. From these factors only volume velocity and heating current can be controlled. Calculations based on empirical correlations show that the temperature difference between the wall and the gas phase at 700 °C is about 5 °C (Sieder and Tate, 1936). In our case the reaction temperature was measured inside the reactor and we suppose that the radial temperature gradient was even smaller. In a tubular flow reactor there is no sharp difference between the preheater and the reactor section. The equivalent volume of the reactor was determined according to Hougen and Watson (1947). All data are related to a reference temperature T_R, "the temperature of the pyrolysis". The equivalent reactor volume V_R is defined as the volume, which gives at the temperature T_R the same conversion as the real reactor with its temperature profile

$$r_{T_R} \cdot dV_R = r_T \cdot dV \tag{2}$$

$$V_R = \frac{1}{\exp\left(-\frac{E}{RT_R}\right)} \cdot \int_0^V \exp\left(-\frac{E}{RT}\right) dV \tag{3}$$

The individual temperature data were measured stepwise (Δl = 2 cm).

The calculated equivalent volume was substituted into the relation for the residence time

$$\tau = \frac{V_R}{(M_F + M_S + M_P)\frac{RT_R}{P}} \tag{4}$$

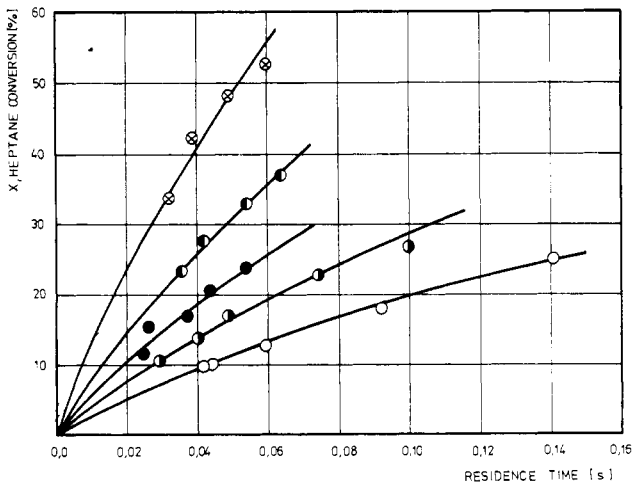

Figure 2. Conversion of *n*-heptane as a function of residence time at different temperatures: ○, 680 °C; ◑, 700 °C; ●, 720 °C; ◐, 740 °C; ⊗, 760 °C.

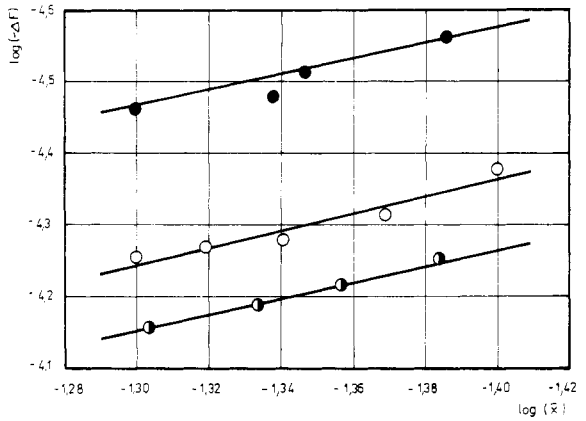

Figure 3. Relation between rate of *n*-heptane consumption and average molar fraction of *n*-heptane at different temperatures: ◑, 680 °C; ○, 700 °C; ●, 720 °C.

Figure 2 shows the relation between conversion and residence time.

Reaction Order

The reaction order was determined according to the method developed by Kershenbaum and Martin (1967). For low conversions the following relation may be derived

$$-\Delta F = \bar{X}^n \left[\frac{QA}{R^n} \int_0^L \exp\left(\frac{-E}{RT(l)}\right)\left(\frac{P(l)}{T(l)}\right)^n \mathrm{d}l \right] \quad (5)$$

At a constant temperature and pressure profile the term in parentheses in eq 5 does not change so that

$$\log(\Delta F) = n \log \bar{X} + \log(\text{constant}) \quad (6)$$

We performed a series of measurements at identical temperature and pressure profiles but with different starting charges of heptane. Relation 5 is shown graphically in Figure 3. The order determined from the graph is 1.01 at 680 °C, 1.02 at 700 °C, and 1.12 at 720 °C.

Rate Constant

Starting from the value of the reaction order, which is approaching one, we assumed for the determination of rate constants and activation energy that the conversion of heptane is governed by a reaction of the first order. For an irreversible reaction we may write

$$A_F + S_W \rightarrow \nu_1 R_1 + \nu_2 R_2 + \nu_3 R_3 + \ldots \nu_i R_i + \ldots + S_W \quad (7)$$

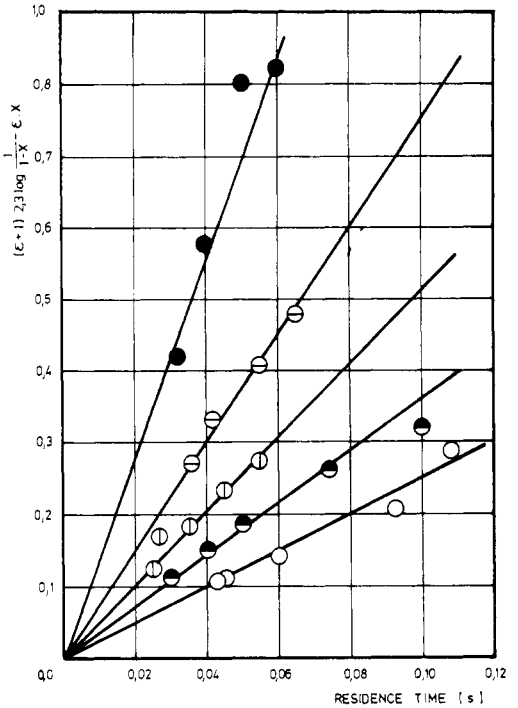

Figure 4. Graphic representation of eq 8 for first-order reaction at different temperatures: ○, 680 °C; ◒, 700 °C; ◑, 720 °C; ⊖, 740 °C; ●, 760 °C.

In a conversion according to eq 7 the steam functions only as an inert diluent. A certain part of this diluent reacts, however, with reaction components according to eq 1. This reaction is negligible, since a large excess of steam is present. For a stationary reactor with plug flow, where an irreversible reaction of the first order proceeds, Levenspiel (1967) derived the following equation

$$k \cdot \tau = (1 + \epsilon) \ln \frac{1}{1 - x} - \epsilon \cdot x \quad (8)$$

ϵ represents the relative change of the volume in the system when passing from zero to complete conversion

$$\epsilon = \frac{V_{x=1} - V_{x=0}}{V_{x=0}} \quad (9)$$

The values of ϵ were determined experimentally. Figure 4 shows the right-hand term of eq 8 as a function of the residence time.

The values of the rate constants as determined graphically from Figure 4 and mean rate constants calculated numerically for five temperatures are listed in Table III. The maximum deviation of numerically derived values is 20.8%. The values of the rate constants in the calculated interval of errors do not show any decreasing trend as a function of the conversion. The same is valid for thermal decomposition of nonane (Kunzru et al., 1972) and 2-pentene (Kunzru et al., 1973) in a tubular reactor from stainless steel. On the contrary in the pyrolysis of heptane in a quartz (Illes et al., 1973; Taniewski and Krajewski, 1975) or brass (Appleby et al., 1947) reactor, the value of the rate constant is decreasing with increasing conversion in consequence of the inhibition by reaction products.

The activation energy calculated from the measured rate constants and determined from the graphical adaptation of the Arrhenius equation (Figure 5) has a value of 195.5 kJ mol^{-1} (46.7 kcal mol^{-1}) and the frequency factor is 1.34 $\times$ 10^{11} s^{-1}. The data available for the activation energy of heptane pyrolysis differ considerably. In a flow system the

Table II. Retention Indices of Pyrolysis Products on a Capillary Squalane Column[a]

	I_{50}		I_{70}		confirmation by MS
	measd	tab. by R-C[d]	measd	tab. by R-C[d]	
1. methane					
2. ethane					
3. propene					
4. propane					
5. methylpropane					
6. 1-butene; 1,3-butadiene					
7. butane					
8. *trans*-2-butene	406.1	406.6			+
9. dimethylpropane	412.5	412.3			
10. *cis*-2-butene	416.3	416.9	416.5	417.3	+
11. 3-methyl-1-butene	450.7	450.3	449.8	450.8	+
12. 1,4-pentadiene	463.8	464.3[b]	464.3	465.0[b]	
13. methylbutane	475.4	475.3	475.0	475.5	
14. 1-pentene	481.5	481.8	481.6	482.1	+
15. 2-methyl-1-butene	488.2	488.0			+
16. *trans*-2-pentene			499.5	499.8	+
17. pentane					
18. *cis*-2-pentene	505.1	504.9	505.9	505.1	+
19. *trans*-1,3-pentadiene	515.7	515.8	516.2	516.5	+
20. 1,3-cyclopentadiene	521.6	521.7[c]			
21. 1,2-pentadiene	525.0	525.6	526.0	525.9	+
22. 2,2-dimethylbutane	536.8	536.8			
23. cyclopentene	549.5	549.5	551.4	552.0	
24. 3-methyl-1-pentene	551.5	551.4	552.9	553.0	
25. 1,5-hexadiene	562.8	562.9	563.3	563.7	
26. 2-methylpentane	569.8	569.7			
27. 2-methyl-1-pentene	580.3	580.1			
28. 1-hexene	582.1	582.3	582.5	582.7	+
29. *trans*-3-hexene	592.4	592.1	591.8	591.6	
30. *trans*-2-hexene	597.0	596.9	596.6	596.7	+
31. hexane					
32. *cis*-2-hexene	603.6	603.6	604.2	604.1	+
33. 3-methyl-*trans*-2-pentene	612.3	612.7	612.8	612.9	
34. *cis*-1,3-hexadiene	622.2	622.0			
35. 2,3-dimethyl-2-butene	624.8	625.1	626.0	625.7	
36. methylcyclopentane	627.8	627.9			
37. benzene	637.2	637.2	642.5	642.0[c]	+
38. 2,4-dimethyl-2-pentene	640.7	640.6			
39. 1-methylcyclopentene	643.8	644.5	646.1	646.8	+
40. 2-methylhexane	666.6	666.6	666.2	667.0	+
41. 3,4-dimethyl-*cis*-2-pentene	670.3	670.6	672.5	671.5	
42. 3-methylhexane	675.5	676.2	676.1	676.9	+
43. 2-methyl-1-hexene	677.5	678.1	678.2	678.5	
44. 1-heptene	681.9	681.8	681.5	682.3	+
45. *cis*-1,3-dimethylcyclopentane	682.9	682.7			
46. 3-methyl-*cis*-3-hexene	684.5	684.6	685.0	685.0	+
47. 3-ethylpentane	686.2	686.0	686.4	687.2	+
48. *trans*-3-heptene	687.6	687.5			+
49. *cis*-3-heptene	690.4	690.4	691.1	691.1	+
50. heptane					
51. *cis*-1,2-dimethylcyclopentane	720.8	720.9	724.2	725.1	+
52. methylcyclohexane	725.8	725.8	730.0	730.6	+
53. 2,4-dimethylhexane	732.5	731.9	733.5	733.0	
54. toluene	744.2	744.3[c]	749.3	749.2[c]	
55. 1-ethylcyclopentene	747.4	747.4[b]			
56. 2-methyl-3-ethylpentane	761.1	761.4			
57. octane					

[a] l = 100 m; i.d. = 0.25 mm; inlet pressure, 2.5 × 10^5 Pa; split ratio, 1:350; number of measurements, 4. [b] Data from Loewenguth and Tourres (1968). [c] Data from Sojak and Rijks (1976). [d] R-C = Rijks and Cramers (1974).

Table III. Rate Constants of the Heptane Conversion

temp, °C	$k_{anal.}$, s^{-1}	std dev at anal. detn, %	k_{graph}, s^{-1}
680	2.28	6.14	2.5
700	3.68	13.58	3.6
720	5.37	20.85	5.2
740	7.64	3.66	7.5
760	14.41	11.72	13.9

thermal decomposition proceeds with an activation energy of 268 kJ mol^{-1} (Appleby et al., 1947), or 216 kJ mol^{-1} (Illes et al., 1973). The first value was found in a brass and the second in a quartz reactor. In static conditions, where the effect of the inner surface is more important, the conversion of heptane in a quartz reactor proceeds with an activation energy of 202 kJ mol^{-1} (Taniewski and Krajewski, 1975). The comparison shows that the pyrolysis of heptane in a tubular reactor from stainless steel with an increased inner surface and in the presence of steam proceeds with the lowest activation energy.

Composition of Reaction Product Mixtures

The average molecular mass of the gaseous products of the pyrolysis varies from 22.4 to 27.3. In this interval the composition of the mixture depends on the temperature

Table IV. Product Distribution in Pyrolysis Mixture of Heptane (mol/100 mol of Heptane Decomposed)

	temp, °C									
	680	680	700	700	720	720	740	740	760	760
	conversion, %									
	9.76	17.9	13.88	26.80	15.51	20.74	23.31	51.03	33.60	52.51
hydrogen	81.13	54.44	51.06	60.40	49.47	47.81	69.59	57.38	116.89	196.27
methane	48.59	53.35	49.52	66.87	44.58	59.30	57.99	61.02	53.62	63.97
ethane	9.18	9.20	6.18	10.01	11.94	12.62	9.23	10.22	15.36	7.87
ethylene	105.96	124.14	116.65	137.75	135.0	148.0	135.22	153.72	144.74	157.23
propane	0.39	1.14	0.84	1.47	1.38	1.10	1.40	1.53	1.15	1.70
propylene	26.23	33.92	31.90	38.24	31.90	35.42	31.00	37.61	24.25	33.82
butane	0.09	0.05	0.49	0.39	0.34	0.29	0.28	0.05	0.17	0.23
1-butene	18.13	26.94	21.30	20.24	19.15	20.04	18.52	16.6	13.78	16.43
trans-2-butene	-	0.25	0.42	0.33	0.37	0.29	0.10	0.41	0.23	0.36
cis-2-butene	-	0.12	0.26	0.37	0.26	0.32	0.69	0.98	0.23	0.35
1,3-butadiene	0.93	2.06	2.63	2.57	2.08	2.49	2.39	4.64	2.68	4.12
3-methylbutene	-	-	0.12	0.23	0.11	0.08	0.07	0.07	0.10	0.11
pentane	-	-	0.32	0.21	0.32	0.08	-	-	-	-
1-pentene	4.89	12.10	13.03	10.09	9.77	9.34	6.20	5.46	6.21	5.20
2-methyl-1-butene	-	-	0.35	0.19	0.21	0.11	-	-	-	-
trans-2-pentene	-	0.09	0.32	0.19	0.22	0.22	0.24	0.32	0.25	0.19
cis-2-pentene	-	0.05	0.25	0.22	0.16	0.15	0.27	0.36	0.25	0.26
1-hexene	4.31	6.24	6.0	5.52	4.79	5.09	4.40	2.78	3.21	1.85
carbon monoxide	27.94	11.73	26.19	12.44	12.48	11.73	21.84	13.13	62.19	24.27

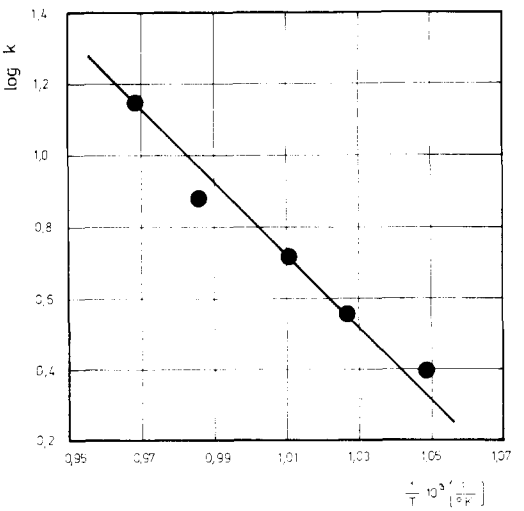

Figure 5. Arrhenius plot for the pyrolysis of *n*-heptane.

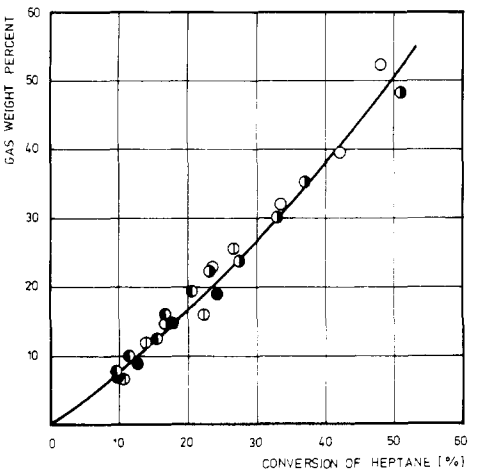

Figure 6. Gas production as a function of conversion of *n*-heptane at different temperatures: ●, 680 °C; ⊙, 700 °C; ◐, 720 °C; ◑, 740 °C; ○, 760 °C.

and the conversion. As expected, the amount of gas from the pyrolysis increases with increasing conversion and the differences recorded between the amounts at a given conversion for different temperatures are insignificant (Figure 6).

Detailed qualitative and quantitative analyses of gaseous and liquid products of the pyrolysis are given in Tables II and IV. Among the liquid and gaseous products of the heptane conversion there are about 55 saturated, olefinic, and aromatic hydrocarbons of different origin. Some of them, viz. methylcyclohexane, 2- and 3-methylhexane, 3-ethylpentane, 1,3- and 1,2-dimethylcyclopentane, 2,4-dimethylhexane, 2-methyl-3-ethylpentane, methylcyclopentane, hexane, and 2-methylpentane are entering into the reactor as impurities with the starting hydrocarbon. The other products are formed by the pyrolysis of heptane.

Under the given conditions ethene is the main product. The yields of ethene, propene, and methane are increasing with an increase in the degree of conversion; the yields of 1-pentene and 1-hexene are decreasing at temperatures above 700 °C. This proves that with extending residence times higher alkanes and olefins are decomposed faster than lower ones. The influence of the residence time on the formation of methane, ethene, propene, 1-butene, 1-pentene, and 1-hexene at 700 °C is shown in Figure 7,

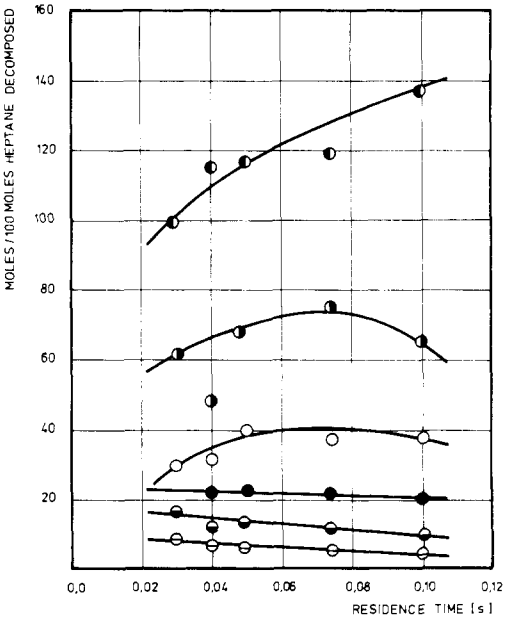

Figure 7. Product distribution vs. residence time of pyrolysis of *n*-heptane at 700 °C: ◐, ethene; ◑, methane; ○, propene; ●, 1-butene; ◒, pentene; ⊖, 1-hexene.

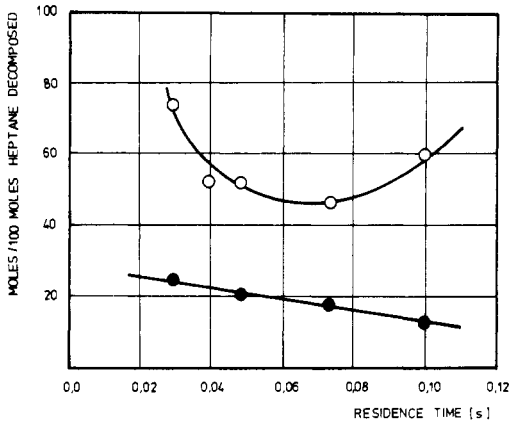

Figure 8. Product distribution vs. residence time of pyrolysis of *n*-heptane at 700 °C: ○, hydrogen; ●, carbon monoxide.

Table V. Comparison of Calculated Yields with Experimental Results in the Pyrolysis of Heptane (mol of Product/100 mol of Heptane Decomposed)

		calcn	expt at 700 °C	
hydrocarbon	Rice-Kossiakoff theory, E = 8.36 kJ	according to Murata and Saito (1973)	according to Murata and Saito (1973)	own results
H_2	---	45	43	51.06
CH_4	53.84	45	47	49.52
C_2H_4	115.38	114	125	116.65
C_2H_6	46.15	11	17	6.18
C_3H_6	30.76	47	44	31.90
1-C_4H_8	15.38	28	27	21.30
1-C_5H_{10}	15.38	19	15	13.03
1-C_6H_{12}	15.38	10	7	6.00
total	292.26	319	326	295.64

and on the formation of hydrogen and carbon monoxide in Figure 8.

Reaction Mechanisms

At present most authors accept the radical mechanism for the thermal decomposition of hydrocarbons. When theoretical rules, which were deduced by Rice (1933) and modified by Kossiakoff and Rice (1943), are applied for the thermal decomposition of heptane, the cracking of the four C_7H_{15} radicals proceeds according to the scheme (A)–(D).

$$CH_3(CH_2)_5\dot{C}H_2 \rightarrow 3C_2H_4 + \dot{C}H_3 \quad (A)$$

$$CH_3(CH_2)_4\dot{C}HCH_3 \rightarrow C_3H_6 + C_2H_4 + \dot{C}_2H_5 \quad (B)$$

$$CH_3(CH_2)_3\dot{C}HCH_2CH_3 \rightarrow C_6H_{12} + \dot{C}H_3 \quad (Ca)$$

$$\rightarrow C_2H_4 + C_4H_8 + \dot{C}H_3 \quad (Cb)$$

$$CH_3(CH_2)_2\dot{C}H(CH_2)_2CH_3 \rightarrow C_5H_{10} + \dot{C}_2H_5 \quad (D)$$

In Table V experimental results are compared with values calculated from the Rice–Kossiakoff theory. At low conversions the yields of ethene and propene agree very well. Comparable results are found also for methane, 1-butene, and 1-pentene. The theoretical prediction highly disagrees in the case of 1-hexene and ethane. In the calculation of the production of 1-hexene it was supposed that the rates of the reactions Ca and Cb are identical. Rice and Kossiakoff showed in their later work that the decomposition via the propyl radical is four times faster than the decomposition to methane and 1-hexene. As the higher olefins are less stable, the produced 1-hexene may be decomposed too via an allylic radical to butadiene

$$CH_2{=}CH\dot{C}HCH_2CH_2CH_3 \rightarrow CH_2{=}CHCH{=}CH_2 + \dot{C}_2H_5 \quad (E)$$

According to Rice and Kossiakoff it is supposed that in the formation of ethane all ethyl radicals (reactions B and D) are reacting intermolecularly with hydrogen or alkane, preferentially with heptane

$$\dot{C}_2H_5 + C_7H_{16} \rightarrow C_2H_6 + \dot{C}_7H_{15} \quad (F)$$

The results obtained under the given conditions disagree with this assumption. A relatively small amount of ethane illustrates the decisive influence of thermodynamic parameters; i.e., temperature and pressure and the catalytic effects of the inner surface of the reactor cannot be ruled out. Thermodynamic data for alkanes with less than six carbon atoms show that higher temperatures and lower pressures are advantageous for dehydrogenation and lower temperatures and higher pressures for hydrogenation. In accordance with the supposition of Rice and Kossiakoff, reaction F is favored at lower temperatures and higher pressures. This is supported by the results of the thermal decomposition of heptane at 580 °C in the absence of inert diluent; for 100 moles of the decomposed starting hydrocarbon 46 moles of ethane are produced, which is in good agreement with 46.15 moles according to the theory (Appleby et al., 1947). The pyrolysis of heptane at temperatures higher than 700 °C and at low partial pressures of reacting components, as a consequence of a high surplus of steam, proceeds in thermodynamically favorable conditions for the dehydrogenation of ethane or ethyl radicals to ethene

$$\dot{C}_2H_5 \rightarrow \dot{C}_2H_4 + H \quad (G)$$

If the assumptions for reaction G are valid, the balance of ethane improves even though the experimental values for the metal reactor with an increased inner surface (Table V, calculation according to Murata and Saito, 1973) are not attained. In this case the amount of ethane is lower than, e.g., from a quartz reactor irrespective of the partial pressure of reacting components, conversion, or kind of the inert diluent. Therefrom it follows that the acceleration of the dehydrogenation according to reaction G may be due to active centers present on the inner wall of the stainless steel reactor.

A referee pointed at an alternative explanation. At lower temperatures, the two reacting species of reaction F are closer together, resulting in a greater number of molecular collisions. Above 700 °C the higher temperature promotes greater separation of these two parts by expansion of the gas. This would give the ethyl radical in reaction F a better chance to collide with a wall and decompose according to reaction G.

The decreased ethane production in the decomposition of heptane in a stainless steel tubular reactor may be ascribed to the catalytic activity of the wall, causing secondary reactions. The nature of these reactions is not obvious. Most probably a portion of the ethyl radicals is converted into methylene and methyl radicals. The methylene radicals may then react, in the presence of metal, with water to form carbon monoxide and hydrogen.

The inner surface of the stainless steel tube displays another characteristic property in the conversion of heptane to methane. The yields of methane are lower than from a quartz reactor (Bajus and Veselý, 1976). In stainless steel a portion of the methyl radicals may be converted to methylene radicals and hydrogen radicals. The methylene radicals may again react with water as described above.

The decreased yields of methane and ethane in a stainless steel reactor are not specific only for the conversion of heptane but occur also with other hydrocarbons, e.g., methylcyclohexane (Bajus et al., 1978), straight-run naphtha, and naphthas from catalytic reforming after extraction of aromatic hydrocarbons (Bajus et al., 1977).

The presence of further products, even if in substantially lower amounts, proves that not only primary reactions are occurring, leading to methane, ethene, light alkanes, and alkenes, but also secondary reactions. The formation of such a rich scale of reaction products proceeds by reactions of cracking, dehydrogenation, isomerization, hydrogenation, polymerization, dehydrocyclization, disproportionation, and condensation. The polymerization and condensation reactions leading to polymeric and especially highly condensed aromatic products of molecular mass higher than that of the starting hydrocarbon are of very minor importance, even if their formation cannot be excluded. The polymers and aromatic products then dehydrogenate to form coke or carbon deposits. The conversion of carbon proceeds according to reaction 1. The reaction products formed by secondary reactions are present in minute amounts and it is difficult to ascertain the extent of the thermal radical process or the catalytic effect of the wall.

Conclusions

The following conclusions can be made from the study of steam pyrolysis of heptane in a laboratory flow reactor with increased inner surface. The inner surface alters the rate of the decomposition. The pyrolysis of heptane proceeds with a relatively small activation energy. The overall decomposition of heptane over the temperature range of 680–760 °C can be assumed to be first order with a frequency factor of 1.34×10^{11} s^{-1} and activation energy 195.5 kJ mol^{-1}. The value of the rate constant was found to be independent of the conversion.

The composition of the reaction product was in agreement with the Rice–Kossiakoff theory except for ethane and 1-hexene. The surface of stainless steel is supposed to act as a catalyst for the decomposition of ethyl radicals into ethene. Part of the ethyl and methyl radicals may be converted into methylene radicals. In an important secondary reaction, carbon or methylene radicals can react in the presence of a metal surface with water to form carbon monoxide and hydrogen.

The detailed qualitative information obtained by gas chromatography (using table matching) and mass spectrometry proves the formation of the rich scale of pyrolysis products by secondary reactions of cracking, dehydrogenation, isomerization, hydrogenation, dehydrocyclization, disproportionation, and condensation.

Nomenclature

$[a]$ = concentration of component, % wt
A = frequency factor for Arrhenius rate expression, s^{-1}
Aa = area of the peak corresponding to a component a, cm^2
$\sum_1^n Ai$ = total area of the peaks, cm^2
A_F = reactant
E = activation energy, kJ mol^{-1}
k = first-order rate constant, s^{-1}
l = reactor length, cm
M_F, M_S, M_P = flow rate of heptane, water (steam) and products, mol s^{-1}
n = order of the reaction
P = pressure, Pa
Q = cross-sectional area of the reactor, cm^2
R = gas constant, J mol^{-1} K^{-1} or m^3 Pa K^{-1} mol^{-1}
R_i = product
S = inner surface of the reactor, cm^2
S_W = steam
T = temperature, K
T_R = reference temperature, K
V = reactor volume, cm^3
V_R = equivalent reactor volume, cm^3
x = conversion of heptane
$\bar{X}$ = average mole fraction of n-heptane
ΔF = rate of heptane consumption, mol h^{-1}

Greek Letters

ϵ = relative volume change in the reaction
τ = residence time, s
ν = moles of product formed per mole of heptane decomposed

Literature Cited

Appleby, W. G.; Avery, W. H.; Meerbott, W. K. *J. Am. Chem. Soc.* **1947**, *69*, 2279.
Bajus, M.; Veselý, V. *Ropa Uhlie* **1976**, *18*, 126.
Bajus, M.; Veselý, V.; Leclercq, P. A.; Rijks, J. A. submitted for publication, 1978.
Bajus, M.; Veselý, V.; Mikulec, J. Symposium Alken 77, Böhlen, March 1–3, 1977.
Crynes, B. L.; Albright, L. F. *Ind. Eng. Chem., Process Des. Dev.* **1969**, *8*, 25.
Hively, R. A.; Hinton, R. E. *J. Gas Chromatogr.* **1968**, *6*, 203.
Hougen, O. A.; Watson, K. M. "Chemical Process Principles", Vol. III; Wiley: New York, 1947; pp 884–886.
Hurd, Ch. D.; Pilgrim, F. D. *J. Am. Chem. Soc.* **1933**, *55*, 4902.
Illes, V.; Welther, K.; Pleszkáts, I. *Acta Chim.* (Budapest) **1973**, *78*, 357.
Kershenbaum, L. S.; Martin, J. J. *AIChEI* **1967**, *13*, 148.
Kossiakoff, A.; Rice, F. O. *J. Am. Chem. Soc.* **1943**, *65*, 580.
Kunzru, D.; Shah, Y. T.; Stuart, E. B. *Ind. Eng. Chem., Process Des. Dev.* **1972**, *11*, 605.
Kunzru, D.; Shah, Y. T.; Stuart, E. B. *Ind. Eng. Chem., Process Des. Dev.* **1973**, *12*, 339.
Leferink, J. G.; Leclercq, P. A. *J. Chromatog.* **1974**, *91*, 385.
Levenspiel, O. "Chemical Reaction Engineering", Teorie a výpocty chemických reaktorov, SNTL: Praha, 1967.
Loewenguth, J. C.; Tourres, D. A. *Z. Anal. Chem.* **1968**, *236*, 170.
Marschner, R. F. *Ind. Eng. Chem.* **1938**, *30*, 554.
Murata, M.; Saito, S. *J. Chem. Eng. Japan* **1973**, *6*, 252.
Rice, F. O. *J. Am. Chem. Soc.* **1933**, *55*, 3035.
Rijks, J. A.; Cramers, C. A. *Chromatographia* **1974**, *7*, 99.
Sieder, E. N.; Tate, G. E. *Ind. Eng. Chem.* **1936**, *28*, 1429.
Soják, L.; Rijks, J. A. *J. Chromatog.* **1976**, *119*, 505.
Tamai, Y.; Nishiyama, Y. *Bull. Jpn. Pet. Inst.* **1970**, *12*, 16.
Tamai, Y.; Nishiyama, Y.; Takahashi, G. *Kogyo Kagaku Zasshi* **1967**, *70*, 889.
Taniewski, M.; Krajewski, J. *Przem. Chem.* **1975**, *54*, 31.
Taylor, J. E.; Hutchings, D. A.; Frech, K. F. *J. Am. Chem. Soc.* **1969**, *91*, 2215.
Tourres, D. A. *J. Chromatog.* **1967**, *30*, 357.

Received for review January 4, 1978
Accepted October 28, 1978

This work was supported by the Scientific Exchange Agreement (S.E.A.).